AN INTEGRAL TRANSFORM SOLUTION FOR UNSTEADY COMPRESSIBLE HEAT TRANSFER IN FLUIDS NEAR THEIR THERMODYNAMIC CRITICAL POINT

by

Leonardo S. de B. ALVES

Laboratory of Theoretical and Applied Mechanics, Department of Mechanical Engineering,
Fluminense Federal University, Niteroi, RJ, Brasil

Original scientific paper
DOI: 10.2298/TSCI120826068D

The classical thermodynamic model for near critical heat transfer is an integral-differential equation with constant coefficients. It is similar to the heat equation, except for a source term containing the time derivative of the bulk temperature. Despite its simple form, analytical methods required the use of approximations to generate solutions for it, such as an approximate Fourier transformation or a numerical Laplace inversion. Recently, the generalized integral transform technique has been successfully applied to this problem, providing a highly accurate analytical solution for it and a new expression of its relaxation time. Nevertheless, very small temperature differences, on the order of mK, have to be imposed so that constant thermal properties can be assumed very close to the critical point. The present paper generalizes this study by relaxing its restriction and accounting for the strong dependence on temperature and pressure of supercritical fluid properties, demonstrating that (a) the generalized integral transform technique can be applied to realistic non-linear unsteady compressible heat transfer in fluids with diverging thermal properties and (b) temperature and pressure have opposite effects on all properties, but their variation causes no additional thermo-acoustic effect, increasing the validity range of the constant property model.

Key words: *piston effect, variable properties, non-linear thermo-acoustics*

Introduction

One measure of fluid compressibility is the ratio between specific heats γ, since it controls the pressure time derivative magnitude in the energy equation. Its smallest possible value is $\gamma = 1$, which represents an incompressible fluid flow. As the fluid's thermodynamic state approaches the critical point, γ diverges and can reach several orders of magnitude [1]. This feature allows small temperature perturbations to create severe compression, which, in turn, generates thermo-acoustic waves. When bounded by solid walls, the subsequent wave propagation and reflection induces a fast heating of the entire fluid, causing a homogeneous increase of its bulk temperature. This phenomenon is known as piston effect and was first observed in low gravity experiments performed inside orbiting rockets [2]. Soon afterwards, the critical speeding-up of temperature relaxation was explained in two alternative ways, using a simple thermodynamic model for entropy generation [3-5] and the Navier-Stokes equations coupled with the van der Waals equation of state [6].

* Authors' e-mail: leonardo.alves@mec.uff.br

The former authors proposed to model the unsteady heat transfer in such a highly compressible fluid under microgravity using the 1-D unsteady heat conduction equations with a source term proportional to the bulk temperature time derivative [3-5]. This term becomes dominant near the critical point ($\gamma \gg 1$) but vanishes in the incompressible limit ($\gamma = 1$). An approximate Fourier transform procedure was employed to solve this model [3], with a detailed description provided elsewhere [5]. This solution considered steady heating at the boundaries in order to reproduce the available experimental data [1]. Nevertheless, it has been extended to pulsed [7] and unsteady [8] heating as well using the same procedure. This model was extended to include two dimensions and curvature effects, introduced by cylindrical container walls [9]. These authors employed separation of variables and Laplace transform with numerical inversion to solve the governing equations.

All these solution procedures required the introduction of some type of approximation to yield analytical expressions. Recently, an exact analytical solution has been obtained using the generalized integral transform technique (GITT) [10], removing the need for any approximations whatsoever. This solution was validated against numerical simulations of the compressible Navier-Stokes equations coupled with an exact differential equation of state [11]. These solutions still considered, however, constant thermodynamic properties, as in all previously cited studies. This restriction limits the maximum amount of heating allowed through the boundary conditions. Although property variations with temperature and pressure have been considered in the past [4], few studies have evaluated their full impact on solution behavior [12]. This latter study considers maximum pressure variations on the order of 25 MPa and maximum temperature variations on the order of 150 K, imposing temperature differences that force the fluid to cross its pseudo-critical lines. However, only a single comparison with a constant property model is presented. It shows a maximum temperature deviation of approximately 2% relative to the maximum temperature difference imposed, despite enormous variations in property values. No explanation is provided for such a small impact, but it is considered enough to justify the need to include property variations. Furthermore, to the best of the author's knowledge, all attempts to find analytical solutions for this problem have been restricted to the use of asymptotic techniques [13-15], but they include property variations with temperature only.

In the present paper, a thermodynamic model for the piston effect that takes into account the temperature and pressure dependence of all fluid properties is solved using the same GITT, extending previous studies that employed constant properties [10, 11]. The two major goals are to (1) explain the roles played by both pressure and temperature dependence of fluid properties on the piston effect and (2) demonstrate that the GITT can also be applied to non-linear versions of the classical model for the unsteady heat transfer taking place under micro-gravity in highly compressible fluids near their thermodynamic critical point. This technique is a generalized version [16] of the classical integral transform technique that evolved from separation of variables [17]. It is a hybrid numerical-analytical solution methodology with global error control that has been applied to many different problems in heat and mass transfer [18]. Finally, it is chosen for the current study due to the successful experience of the author in using it to simulate natural convection in porous media [19], non-linear convection-diffusion flows [20], and Rayleigh-Benard instability in porous media [21].

Problem formulation

It will be considered here a 1-D cavity of length L placed in a zero gravity environment and filled with single phase CO_2 at an initial state close to the critical point, defined by NIST as $T_C = 304.1282$ K and $P_C = 7.3773$ MPa. Both left and right impermeable wall temperatures are

suddenly raised by the exact same amount in order to initiate the supercritical heat transfer process. This is a canonical problem in thermo-acoustic heat transfer because a strong piston effect inhibits thermal diffusion, essentially isolating its effect on the bulk temperature relaxation process.

Mathematical model

The governing equations for this problem are taken from [4], which simplify to equations given by [3, 5] in the constant properties limit. There are two equations. One is obtained from energy conservation, where entropy changes are balanced by thermal diffusion. It is given by:

$$\overline{\rho}\overline{C}_{\mathrm{P}}\frac{\partial\overline{T}}{\partial\overline{t}}-\overline{\rho}(\overline{C}_{\mathrm{P}}-\overline{C}_{\mathrm{V}})\frac{\overline{\kappa}_{\mathrm{T}}}{\overline{\alpha}_{\mathrm{P}}}\frac{\partial\overline{P}}{\partial\overline{t}}=\frac{\partial}{\partial\overline{x}}\left(\overline{k}\frac{\partial\overline{T}}{\partial\overline{x}}\right) \tag{1}$$

with the over bar indicating a dimensional form. In eq. (1), T is the temperature, P – the pressure, x and t are the spatial and temporal co-ordinates, ρ is the density, C_{P} and C_{V} are the specific heats at constant pressure and volume, k is the thermal conductivity, κ_{T} and α_{P} are the isothermal compressibility and volumetric thermal expansion coefficients, defined, respectively, as:

$$\overline{\kappa}_{\mathrm{T}}=\frac{1}{\overline{\rho}}\frac{\partial\overline{\rho}}{\partial\overline{P}}\bigg|_{\mathrm{T}}\quad\text{and}\quad\overline{\alpha}_{\mathrm{P}}=-\frac{1}{\overline{\rho}}\frac{\partial\overline{\rho}}{\partial\overline{T}}\bigg|_{\mathrm{P}} \tag{2}$$

On the other hand, the other equation is obtained from mass conservation, written as a total differential for density. It is given by:

$$\frac{\partial\overline{\rho}}{\partial\overline{t}}=\overline{\rho}\overline{\kappa}_{\mathrm{T}}\frac{\partial\overline{P}}{\partial\overline{t}}-\overline{\rho}\overline{\alpha}_{\mathrm{P}}\frac{\partial\overline{T}}{\partial\overline{t}} \tag{3}$$

when divided by dt, since this is a very low Mach number flow and natural convection does not set in. One should note that the fluid mass within the cavity does not vary. Hence, it is possible to integrate eq. (2) over the constant cavity volume to generate:

$$\frac{\partial\overline{P}}{\partial\overline{t}}=\frac{\int_0^L\overline{\rho}\overline{\alpha}_{\mathrm{P}}\dfrac{\partial\overline{T}}{\partial\overline{t}}\mathrm{d}\overline{x}}{\int_0^L\overline{\rho}\overline{\kappa}_{\mathrm{T}}\mathrm{d}\overline{x}} \tag{4}$$

where all properties in eqs. (1) and (2) are temperature and pressure dependent. Furthermore, eq. (4) is written in this way because pressure was assumed to depend only on time. Spatial variations are negligible since pressure waves travel at an acoustic time scale, which is much smaller than the other two relevant time scales in the current problem, t_{D} and t_{PE}, *i. e.*, thermal diffusion and piston effect time scales, respectively. It is important to note that eq. (4) cannot be substituted into eq. (1) because all thermodynamic properties depend not only on temperature but on pressure as well. Initial and boundary conditions for this problem are given by:

$$\overline{P}(\overline{t}=0)=\overline{P}_0,\quad\overline{T}(\overline{x},\overline{t}=0)=\overline{T}_0,\quad\overline{T}(\overline{x}=0,\overline{t})=\overline{T}_1,\quad\text{and}\quad\overline{T}(\overline{x}=L,\overline{t})=\overline{T}_1 \tag{5}$$

Dimensionless governing equations

Subscripts as well as superscripts 0 and C represent a property evaluated at the initial state, defined by T_0 and P_0, and the critical state, defined by T_{C} and P_{C}, respectively. All thermodynamic properties are made dimensionless through their respective value at the initial state and written as:

$$\rho = \frac{\overline{\rho}}{\overline{\rho}_0},\ C_{\mathrm{P}} = \frac{\overline{C}_{\mathrm{P}}}{\overline{C}_{\mathrm{P}}^{0}},\ C_{\mathrm{V}} = \frac{\overline{C}_{\mathrm{V}}}{\overline{C}_{\mathrm{V}}^{0}},\ \kappa_{\mathrm{T}} = \overline{\kappa}_{\mathrm{T}}\overline{P}_C,\quad \alpha_{\mathrm{P}} = \overline{\alpha}_{\mathrm{P}}\overline{T}_{\mathrm{C}},\ \text{and}\ k = \frac{\overline{k}}{\overline{k}_0} \tag{6}$$

and the remaining variables and parameters are written in dimensionless form as:

$$T = \frac{\overline{T} - \overline{T}_{\mathrm{C}}}{\overline{T}_{\mathrm{C}}},\ P = \frac{\overline{P} - \overline{P}_{\mathrm{C}}}{\overline{P}_{\mathrm{C}}},\ x = \frac{\overline{x}}{L},\ t = \frac{\overline{t}}{\frac{L^2}{\alpha_0}},\ \alpha_0 = \frac{\overline{k}_0}{\overline{\rho}_0\overline{C}_{\mathrm{P}}^{0}},\ \text{and}\ \gamma_0 = \frac{\overline{C}_{\mathrm{P}}^{0}}{\overline{C}_{\mathrm{V}}^{0}} \tag{7}$$

where α_0 is the thermal diffusivity and γ_0 – the specific heat ratio, both evaluated at the initial state. It is important to note that dimensionless forms for temperature and pressure follow the standard choice in supercritical heat transfer, measuring a distance from the critical point associated with the universal divergence phenomenon [1]. Now, eqs. (1) and (3) become, respectively:

$$\rho C_{\mathrm{P}}\frac{\partial T}{\partial t} - \rho\left(C_{\mathrm{P}} - \frac{C_{\mathrm{V}}}{\gamma_0}\right)\frac{\kappa_{\mathrm{T}}}{\alpha_{\mathrm{P}}}\frac{\mathrm{d}P}{\mathrm{d}t} = \frac{\partial}{\partial x}\left(k\frac{\partial T}{\partial x}\right) \tag{8}$$

$$\frac{\partial P}{\partial t} = \frac{\int_0^1 \rho\alpha_{\mathrm{P}}\frac{\partial T}{\partial t}\mathrm{d}x}{\int_0^1 \rho\kappa_{\mathrm{T}}\mathrm{d}x} \tag{9}$$

with dimensionless symbols written without the over bar. Initial and boundary conditions imposed in eq. (5) are now written as:

$$P(t=0) = P_0,\quad T(x,t=0) = T_0,\quad T(x=0,t) = T_1,\quad \text{and}\quad T(x=1,t) = T_1 \tag{10}$$

where the new parameters that naturally appear are defined as:

$$P_0 = \frac{\overline{P}_0 - \overline{P}_{\mathrm{C}}}{\overline{P}_{\mathrm{C}}},\ T_0 = \frac{\overline{T}_0 - \overline{T}_{\mathrm{C}}}{\overline{T}_{\mathrm{C}}},\ \text{and}\ T_1 = \frac{\overline{T}_1 - \overline{T}_{\mathrm{C}}}{\overline{T}_{\mathrm{C}}} \tag{11}$$

Thermodynamic properties

As already mentioned in the subsection *Mathematical model*, all thermodynamic properties in the present study depend on both temperature and pressure. In order to model this dependence, temperature and pressure changes away from each initial state are considered small enough for a linear dependence to be accurate. Hence, it will be assumed here the following relations:

$$\rho = 1 - \alpha_{\mathrm{P}}^{0}(T - T_0) + \kappa_{\mathrm{T}}^{0}(P - P_0) \tag{12}$$

$$C_{\mathrm{P}} = 1 + \left.\frac{\partial C_{\mathrm{P}}}{\partial T}\right|_0 (T - T_0) + \left.\frac{\partial C_{\mathrm{P}}}{\partial P}\right|_0 (P - P_0) \tag{13}$$

$$C_{\mathrm{V}} = 1 + \left.\frac{\partial C_{\mathrm{V}}}{\partial T}\right|_0 (T - T_0) + \left.\frac{\partial C_{\mathrm{V}}}{\partial P}\right|_0 (P - P_0) \tag{14}$$

$$\kappa_{\mathrm{T}} = \kappa_{\mathrm{T}}^{0} + \left.\frac{\partial \kappa_{\mathrm{T}}}{\partial T}\right|_0 (T - T_0) + \left.\frac{\partial \kappa_{\mathrm{T}}}{\partial P}\right|_0 (P - P_0) \tag{15}$$

$$\alpha_{\mathrm{P}} = \alpha_{\mathrm{P}}^{0} + \left.\frac{\partial \alpha_{\mathrm{P}}}{\partial T}\right|_0 (T - T_0) + \left.\frac{\partial \alpha_{\mathrm{P}}}{\partial P}\right|_0 (P - P_0) \tag{16}$$

$$k = 1 + \left.\frac{\partial k}{\partial T}\right|_0 (T - T_0) + \left.\frac{\partial k}{\partial P}\right|_0 (P - P_0) \tag{17}$$

where C_P and α_P have the strongest property divergences, followed closely by κ_T. On the other hand, the property divergence of k is much weaker, with ρ and C_V being the weakest. The new parameters that naturally appear are defined as:

$$\alpha_P^0 = \overline{\alpha}_P^0 \overline{T}_C \quad \text{and} \quad \kappa_T^0 = \overline{\kappa}_T^0 \overline{P}_C \tag{18}$$

Solving governing eqs. (8) and (9) subject to linearized properties (12) to (17) leads to strong non-linearities in the resulting equations. They are, however, not entirely necessary. As will be noted in the next section, they create a coupling in the temperature time derivative of eq. (8) that dramatically increases the required computer time to solve it. Such a problem was avoided in eq. (9) due to the fact that pressure is time dependent only. Furthermore, both equations can be manipulated in such a way to decrease the order of the non-linear terms. In essence, it is possible to re-write this system as:

$$\frac{\partial T}{\partial t} = \frac{1}{\rho C_P} \frac{\partial}{\partial x}\left(k \frac{\partial T}{\partial x} \right) + \left(1 - \frac{1}{\gamma_0} \frac{C_V}{C_P} \right) \frac{\kappa_T}{\alpha_P} \frac{\mathrm{d}P}{\mathrm{d}t} \tag{19}$$

$$\frac{\partial P}{\partial t} = \frac{\int_0^1 \rho \alpha_P \frac{\partial T}{\partial t} \mathrm{d}x}{\int_0^1 \rho \kappa_T \mathrm{d}x} \tag{20}$$

with linearization applied directly to the property combinations $1/(\rho C_P)$, C_V/C_P, κ_T/α_P, $\rho\alpha_P$, and $\rho\kappa_T$, instead of each individual property, around reference initial state P_0 and T_0. In other words, based on eqs. (12) to (16), these property combinations are written as:

$$\frac{1}{\rho C_P} = 1 + \phi_T^1 (T - T_0) + \phi_P^1 (P - P_0) \tag{21}$$

$$\frac{C_V}{C_P} = 1 + \phi_T^2 (T - T_0) + \phi_P^2 (P - P_0) \tag{22}$$

$$\frac{\kappa_T}{\alpha_P} = \frac{\kappa_T^0}{\alpha_P^0} [1 + \phi_T^3 (T - T_0) + \phi_P^3 (P - P_0)] \tag{23}$$

$$\rho\alpha_P = \alpha_P^0 [1 + \phi_T^4 (T - T_0) + \phi_P^4 (P - P_0)] \tag{24}$$

$$\rho\kappa_T = \kappa_T^0 [1 + \phi_T^5 (T - T_0) + \phi_P^5 (P - P_0)] \tag{25}$$

and used with eq. (17) for thermal conductivity. Constants ϕ_T^i and ϕ_P^i represent rate of change with respect to temperature and pressure, respectively. Property dependences on temperature and pressure are shown in figs. 1 to 4, which include near critical states on both sides of the pseudo-critical line. This feature leads to opposite temperature and pressure dependences between figs. 1 and 2 as well as 3 and 4. Furthermore, it is clear that a linear dependence of all properties on both temperature and pressure reproduces reasonably well the experimental data, represented by symbols, within the ranges shown. These ranges are 1 K in the first two figures and 100 mK in the last two. Pressure ranges in these figures are approximately 326, 99.2, 12.0, and 23.8 kPa. These temperature differences are exactly imposed through their boundary condi-

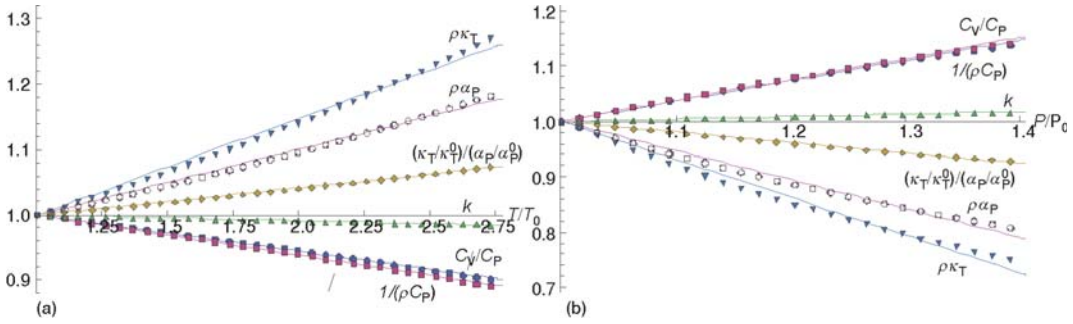

Figure 1. CO_2 properties, presented in eqs. (17) and (21) to (25), dependences on (a) temperature at P_0 = 8.4 MPa and (b) pressure at T_0 = 304.7 K

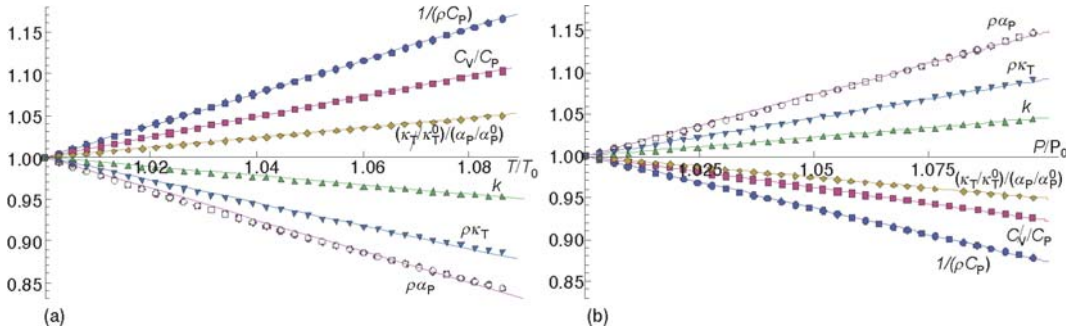

Figure 2. CO_2 properties, presented in eqs. (17) and (21) to (25), dependences on (a) temperature at P_0 = 8.4 MPa and (b) pressure at T_0 = 315.615 K

tions in eq. (10) whereas their respective pressure differences are a direct consequence of eq. (20). Initial states are shown in each figure, but it is important to mention that $\gamma_0 \approx 5$ for the first two and $\gamma_0 \approx 15.5$ for the last two. Hence, these four cases represent not only two different qualitative dependences of thermodynamic properties on both temperature and pressure but also two different overall compressibility levels.

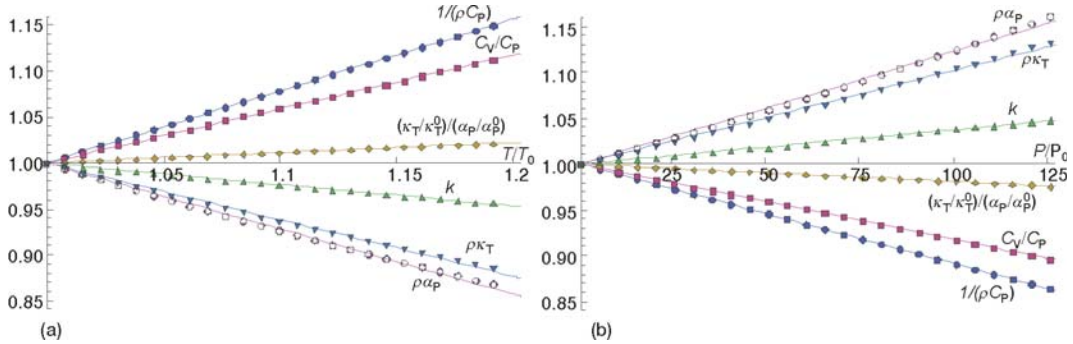

Figure 3. CO_2 properties, presented in eqs. (17) and (21) to (25), dependences on (a) temperature at P_0 = 7.3774 MPa and (b) pressure at T_0 = 304.65 K

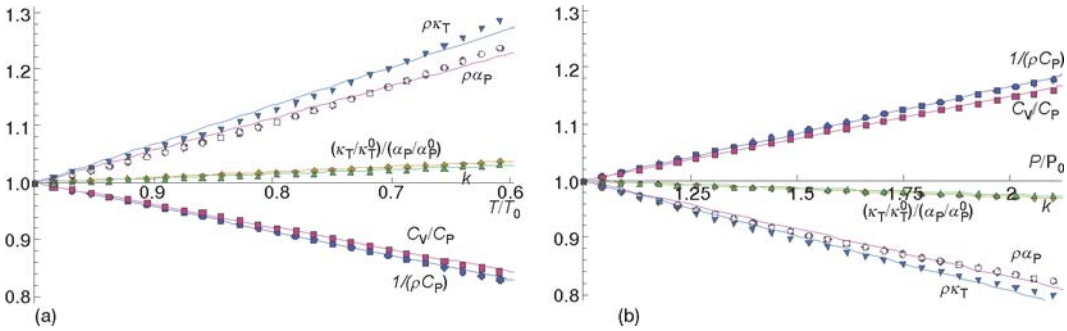

Figure 4. CO_2 properties, presented in eqs. (17) and (21) to (25), dependences on (a) temperature at P_0 = 7.4 MPa and (b) pressure at T_0 = 303.873 K

Solution methodology

Equations (19) and (20), with initial and boundary conditions (10) and using combined property dependences (21) to (25) as well as property (17) (see figs. 1 to 4), form the system of equations that governs the unsteady near critical heat transfer process. This system of equations is solved using the GITT. This approach analytically removes the spatial dependence of the unsteady governing equations, transforming them into a system of transient ordinary differential equations. At this point, well established numerical methods can be employed to march this initial value problem in time. The original profile is then recovered through a pre-determined analytical inversion formula. A detailed discussion is presented next.

Filter

An important first step, which can be considered part of the methodology itself, is the introduction of a filter. The integral transformation process, described in the next subsection, utilizes a base function for the spatial integration that is obtained from a homogeneous eigenvalue problem. Hence, non-homogeneous boundary conditions in eq. (10) have a deleterious effect on the series solution convergence, which is known as Gibbs phenomenon. For this reason, it is useful to employ relation:

$$T(x,t) = T_{\mathrm{F}}(x) + \theta(x,\, t) \tag{26}$$

where T_{F} is the filter chosen to make the boundary conditions in eq. (10) homogeneous, given by:

$$T_{\mathrm{F}}(x)=T_1 \tag{27}$$

and θ represents the new homogeneous temperature field. Now, relation (26) can be substituted into the original non-homogenous system of eqs. (19) and (20), leading to:

$$\frac{\partial\theta}{\partial t} = \frac{1}{\rho C_P}\frac{\partial}{\partial x}\left(k\frac{\partial\theta}{\partial x}\right)+\left(1-\frac{1}{\gamma_0}\frac{C_{\mathrm{V}}}{C_{\mathrm{P}}}\right)\frac{\kappa_{\mathrm{T}}}{\alpha_{\mathrm{P}}}\frac{\mathrm{d}P}{\mathrm{d}t} \tag{28}$$

$$\frac{\partial P}{\partial t} = \frac{\int_0^1 \rho\alpha_{\mathrm{P}}\dfrac{\partial\theta}{\partial t}\mathrm{d}x}{\int_0^1 \rho\kappa_{\mathrm{T}}\mathrm{d}x} \tag{29}$$

which is subject to the new initial and homogeneous boundary conditions:

$$P(t=0)=P_0,\quad \theta(x,\,t=0)=-\Delta T=T_0-T_1,\quad \theta(x=0,\,t)=\theta(x=1,\,t)=0 \tag{30}$$

Generalized integral transform technique

A series solution for homogeneous temperature can now be proposed in the form:

$$\theta(x,t)=\sum_{i=1}^{N}\widetilde{\psi}_i(x)\widetilde{\theta}_i(t) \tag{31}$$

where the eigenfunctions arise from the Sturm-Liouville problem:

$$\frac{\mathrm{d}^2\psi_i}{\mathrm{d}x^2}+\beta_i^2\psi_i(x)=0,\quad \psi_i(0)=0,\quad \text{and}\quad \psi_i(1)=0 \tag{32}$$

whose boundary conditions are also homogenous as in eq. (30). This problem yields:

$$\psi_i(x)=\sin(\beta_i x)\quad \text{and}\quad \beta_i=i\pi \tag{33}$$

for the eigenfunctions and eigenvalues, respectively, with i = 1, 2,…, N. Since these eigenfunctions are orthogonal, the integral transformed homogeneous temperature can be defined as:

$$\widetilde{\theta}_i(t)=\int_0^1\widetilde{\psi}_t(x)\theta(x,t)\,\mathrm{d}x \tag{34}$$

using the normalized eigenfunctions employed in eq. (31), related to the eigenfunctions through:

$$\widetilde{\psi}_i(x)=\frac{\psi_i(x)}{\sqrt{N_i}}\quad \text{with}\quad N_i=\int_0^1\psi_i^2(x)\,\mathrm{d}x=\frac{1}{2} \tag{35}$$

defining the norm. It is important to mention that, although $N=\infty$ in theory, N only has to be made large enough in order to guarantee a user prescribed error tolerance for the convergent series (31).

Having established the integral/transform pair in eqs. (31) and (34), it is now possible to proceed with the integral transformation procedure. First, substituting eqs. (17) and (21) to (25) into eqs. (28) and (29) allows these latter equations to be re-written as:

$$\begin{aligned}\frac{\partial\theta}{\partial t}=&[1+\phi_{\mathrm{T}}^1(\theta+\Delta T)+\phi_{\mathrm{P}}^1(P-P_0)]\frac{\partial}{\partial x}\left\{[1+\phi_{\mathrm{T}}^0(\theta+\Delta T)+\phi_{\mathrm{P}}^0(P-P_0)]\frac{\partial\theta}{\partial x}\right\}+\\&+\left\{1-\frac{1}{\gamma_0}[1+\phi_{\mathrm{T}}^2(\theta+\Delta T)+\phi_{\mathrm{P}}^2(P-P_0)]\right\}[1+\phi_{\mathrm{T}}^3(\theta+\Delta T)+\phi_{\mathrm{P}}^3(P-P_0)]\frac{\kappa_{\mathrm{T}}^0}{\alpha_{\mathrm{P}}^0}\frac{\mathrm{d}P}{\mathrm{d}t}\end{aligned} \tag{36}$$

and

$$\frac{\kappa_{\mathrm{T}}^0}{\alpha_{\mathrm{P}}^0}\frac{\partial P}{\partial t}=\frac{\int_0^1[1+\phi_{\mathrm{T}}^4(\theta+\Delta T)+\phi_{\mathrm{P}}^4(P-P_0)\dfrac{\partial\theta}{\partial t}\,\mathrm{d}x}{\int_0^1[1+\phi_{\mathrm{T}}^5(\theta+\Delta T)+\phi_{\mathrm{P}}^5(P-P_0)\,\mathrm{d}x} \tag{37}$$

where $\phi_{\mathrm{T}}^0=\partial k/\partial T$ and $\phi_{\mathrm{P}}^0=\partial k/\partial P$ evaluated at T_0 and P_0 in eq. (17). Once again, this system can be re-written, but now in an expanded form, as:

$$\begin{aligned}\frac{\partial\theta}{\partial t}=&\frac{\partial^2\theta}{\partial x^2}+\left(1-\frac{1}{\gamma_0}\right)\frac{\kappa_{\mathrm{T}}^0}{\alpha_{\mathrm{P}}^0}\frac{\mathrm{d}P}{\mathrm{d}t}+a_1\frac{\partial^2\theta}{\partial x^2}+a_2\left(\frac{\partial\theta}{\partial x}\right)^2+a_3\theta\frac{\partial^2\theta}{\partial x^2}+\\&+a_4\theta\left(\frac{\partial\theta}{\partial x}\right)^2+a_5\theta^2\frac{\partial^2\theta}{\partial x^2}+(b_1+b_2\theta-b_3\theta^2)\frac{\kappa_{\mathrm{T}}^0}{\alpha_{\mathrm{P}}^0}\frac{\mathrm{d}P}{\mathrm{d}t}\end{aligned} \tag{38}$$

and

$$(1+d_1+d_2\theta_b)\frac{\kappa_{\mathrm{T}}^0}{\alpha_{\mathrm{P}}^0}\frac{\mathrm{d}P}{\mathrm{d}t}=(1+c_1)\frac{\mathrm{d}\theta_{\mathrm{b}}}{\mathrm{d}t}+c_2\int_0^1\theta\frac{\partial\theta}{\partial t}\mathrm{d}x \tag{39}$$

in order to highlight the additional terms due to the property dependence on temperature and pressure, multiplied here by a_i, b_i, c_i, and d_i. Furthermore, it is important to define:

$$T_{\mathrm{b}}(t)=T_1+\theta_{\mathrm{b}}(t)\quad\text{where}\quad\theta b(t)=\int_0^1\theta(x,t)\mathrm{d}x \tag{40}$$

as the bulk temperature, since θ_{b} appears in eq. (39). The coefficients associated with these terms, which can be time dependent since they can contain pressure, are given by:

$$\begin{gathered}a_1=(1+\phi_{\mathrm{T}}^0\Delta T+\phi_{\mathrm{P}}^0\Delta P)(1+\phi_{\mathrm{T}}^1\Delta T+\phi_{\mathrm{P}}^1\Delta P)-1,\quad a_2=\phi_{\mathrm{T}}^0(1+\phi_{\mathrm{T}}^1\Delta T+\phi_{\mathrm{P}}^1\Delta P)\\ a_3=a_2+\phi_{\mathrm{T}}^1(1+\phi_{\mathrm{T}}^0\Delta T+\phi_{\mathrm{P}}^0\Delta P),\quad\text{and}\quad a_4=a_5=\phi_{\mathrm{T}}^0\phi_{\mathrm{T}}^1\end{gathered} \tag{41}$$

$$\begin{gathered}b_1=(1-\gamma_0^{-1})(\phi_{\mathrm{T}}^3\Delta T+\phi_{\mathrm{P}}^3\Delta P)-\gamma_0^{-1}(\phi_{\mathrm{T}}^2\Delta T+\phi_{\mathrm{P}}^2\Delta P)(\phi_{\mathrm{T}}^3\Delta T+\phi_{\mathrm{P}}^3\Delta P),\\ b_2=\phi_{\mathrm{T}}^3[1-\gamma_0^{-1}(1+\phi_{\mathrm{T}}^2\Delta T+\phi_{\mathrm{P}}^2\Delta P)]-\phi_{\mathrm{T}}^2(1+\phi_{\mathrm{T}}^3\Delta T+\phi_{\mathrm{P}}^3\Delta P),\quad\text{and}\quad b_3=\phi_{\mathrm{T}}^2\phi_{\mathrm{T}}^3\end{gathered} \tag{42}$$

$$c_1=\phi_{\mathrm{T}}^4\Delta T+\phi_{\mathrm{P}}^4\Delta P\quad\text{and}\quad c_2=\phi_{\mathrm{T}}^4 \tag{43}$$

$$d_1=\phi_{\mathrm{T}}^5\Delta T+\phi_{\mathrm{P}}^5\Delta P\quad\text{and}\quad d_2=\phi_{\mathrm{T}}^5 \tag{44}$$

where $\Delta P=P(t)-P_0$. Multiplying eq. (38) by the normalized eigenfunction (35), integrating the result over the cavity length and utilizing transformation (34) where possible leads to:

$$\begin{gathered}\frac{\mathrm{d}\widetilde{\theta}_i}{\mathrm{d}t}=[(1+b_1)\eta_i+b_2\widetilde{\theta}_i]\left(1-\frac{1}{\gamma_0}\right)\frac{\kappa_{\mathrm{T}}^0}{\alpha_{\mathrm{P}}^0}\frac{\mathrm{d}P}{\mathrm{d}t}-(1+a_1)\beta_i^2\widetilde{\theta}_i+\\ +\int_0^1\widetilde{\psi}_i\left[a_2\left(\frac{\partial\theta}{\partial x}\right)^2+a_3\theta\frac{\partial^2\theta}{\partial x^2}-b_3\theta^2\frac{\kappa_{\mathrm{T}}^0}{\alpha_{\mathrm{P}}^0}\frac{\mathrm{d}P}{\mathrm{d}t}+a_4\theta\left(\frac{\partial\theta}{\partial x}\right)^2+a_5\theta^2\frac{\partial^2\theta}{\partial x^2}\right]\mathrm{d}x\end{gathered} \tag{45}$$

where the linear diffusion term was integrated by parts, with eq. (32) substituted in the results before transformation (34) is employed [17]. The second line in eq. (45) includes all terms that cannot be integral transformed in the classical sense. In order to overcome this difficulty [16,18], one must substitute inverse eq. (31) into eq. (45) to obtain:

$$\begin{gathered}\frac{\mathrm{d}\widetilde{\theta}_i}{\mathrm{d}t}=[(1+b_1)\eta_i+b_2\widetilde{\theta}_i]\left(1-\frac{1}{\gamma_0}\right)\frac{\kappa_{\mathrm{T}}^0}{\alpha_{\mathrm{P}}^0}\frac{\mathrm{d}P}{\mathrm{d}t}-(1+a_1)\beta_i^2\widetilde{\theta}_i+\\ +\sum_{j=1}^N\sum_{k=1}^N B_{i,j,k}\widetilde{\theta}_j\widetilde{\theta}_k+\sum_{j=1}^N\sum_{k=1}^N\sum_{m=1}^N C_{i,j,k,m}\widetilde{\theta}_j\widetilde{\theta}_k\widetilde{\theta}_m\end{gathered} \tag{46}$$

for $i = 1, 2,\ldots, N$. Pressure is obtained from eq. (39), which can be written as:

$$(1+d_1+d_2\sum_{j=1}^N\eta_j\widetilde{\theta}_j)\frac{\kappa_{\mathrm{T}}^0}{\alpha_{\mathrm{P}}^0}\frac{\mathrm{d}P}{\mathrm{d}t}=(1+c_1)\sum_{j=1}^N\eta_j\frac{\mathrm{d}\widetilde{\theta}_j}{\mathrm{d}t}+c_2\sum_{j=1}^N\sum_{k=1}^N A_{j,k}\widetilde{\theta}_j\frac{\mathrm{d}\widetilde{\theta}_k}{\mathrm{d}t} \tag{47}$$

if eq. (31) is substituted into it as well. The integral coefficients in these coupled system are:

$$\eta_i=\int_0^1\widetilde{\psi}_i\mathrm{d}x,\quad A_{i,j}=\int_0^1\widetilde{\psi}_i\widetilde{\psi}_j\mathrm{d}x$$

$$B_{i,j,k}=a_2\int_0^1\widetilde{\psi}_i\frac{\mathrm{d}\widetilde{\psi}_j}{\mathrm{d}x}\frac{\mathrm{d}\widetilde{\psi}_k}{\mathrm{d}x}\mathrm{d}x+a_3\int_0^1\widetilde{\psi}_i\widetilde{\psi}_j\frac{\mathrm{d}^2\widetilde{\psi}_k}{\mathrm{d}x^2}\mathrm{d}x-b_3\frac{\kappa_{\mathrm{T}}^0}{\alpha_{\mathrm{P}}^0}\frac{\mathrm{d}P}{\mathrm{d}t}\int_0^1\widetilde{\psi}_i\widetilde{\psi}_j\widetilde{\psi}_k\mathrm{d}x$$

$$C_{i,j,k,m} = a_4 \int_0^1 \widetilde{\psi}_i \widetilde{\psi}_j \frac{\mathrm{d}\widetilde{\psi}_k}{\mathrm{d}x} \frac{\mathrm{d}\widetilde{\psi}_m}{\mathrm{d}x} \mathrm{d}x + a_5 \int_0^1 \widetilde{\psi}_i \widetilde{\psi}_j \widetilde{\psi}_k \frac{\mathrm{d}^2\widetilde{\psi}_m}{\mathrm{d}x^2} \mathrm{d}x \tag{48}$$

where all integrals yield analytical results. Equations (46) and (47) are subject to initial conditions:

$$P(t=0) = P_0 \quad \text{and} \quad \widetilde{\theta}_i(t=0) = -\eta_i \Delta T \tag{49}$$

for $i = 1, 2, \ldots, N$. The latter expression is obtained by a similar procedure. First, one multiplies the temperature initial condition in eq. (30) by the normalized eigenfunction (35), integrates the result over the cavity length and utilizes transformation (34) and integral coefficient η_i in (48). It is important to mention that the classical linear system [10, 11] is recovered if one sets $a_i = b_i = c_i = d_i = 0$ and substitutes eq. (47) into eq. (46). Now, system of equations (46) to (49) can be simulated with a reliable numerical solver for ordinary differential equations. The solution for pressure becomes readily available and eqs. (26) and (31) can be utilized to generate the solution for temperature.

Results and discussions

Numerical procedure

Although the solution for temperature is based on the known analytical expressions (26) and (31), where the spatial dependence of the latter is based on the known analytical eigenvalues and eigenfunctions in (33), the transformed temperature dependence on time must be obtained numerically due to the coupling introduced by the non-linear terms in eq. (46). Since this system of equations is coupled with eq. (47), pressure, which depends on time only, must also be obtained numerically. This is achieved with the built-in function NDSolve of the software Mathematica [22] using 18 digits for the calculations to guarantee a minimum of 9 digits in both absolute and relative errors.

Furthermore, the coupling between transformed temperature and pressure, as was written in eqs. (46) and (47), introduces quite significant cancellation errors. In order to overcome this problem, an iterative solution procedure was employed. First, pressure is assumed constant and equal to its initial value. Equation (46) is then solved for the transformed temperature. Now, a new solution for pressure can be generated from eq. (47) using this solution just obtained for the transformed temperature. This process is repeated until the maximum pressure absolute error is smaller than 10^{-6}, where it is important to note that respective relative errors are of the same order of magnitude. Figure 5 shows (a) the decay in maximum relative error per iteration for $N =$

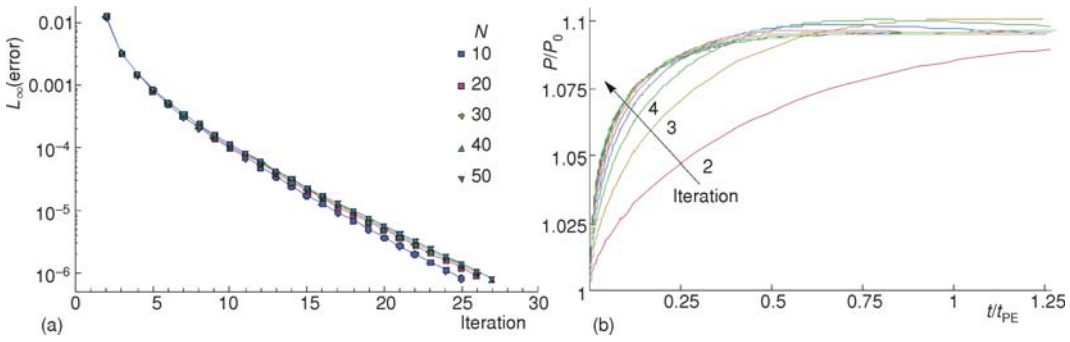

Figure 5. Pressure (a) maximum absolute error *vs.* iteration and (b) time dependence at $N = 30$

10, 20, …, 50 as well as (b) the pressure dependence on time, re-scaled with $t_{PE} = \gamma_0^{-1}$ [10, 11], for each iteration and $N = 30$. All data presented in this figure refers to the thermodynamic conditions reported in fig. 2. It can be observed that the maximum error occurs at a very small but non-zero time and decreases as time increases. Furthermore, both errors in magnitude and position become smaller than 1% between 8 ≤ Iteration ≤ 10. This procedure, however, becomes quite slow as N increases because the number of iterations required for convergence changes very little with N, as shown in fig. 5(a). Hence, an alternative segregated procedure is utilized instead. An initial solution for temperature and pressure is first obtained from eqs. (46) and (47) with $N = 1$. The loop is then started at $N = 2$, where eq. (46) is solved for temperature using the pressure field generated with $N = 1$. The next step updates pressure by solving eq. (47) using the temperature field generated with $N = 2$ in the previous step. N is increased by one and the loop is repeated until the aforementioned stopping criteria is reached. In essence, a solution from this procedure with N terms is as accurate as the solution from the previous procedure with $N - 1$ terms. However, this new procedure requires a significantly smaller computer time.

Series solution convergence

Now that the accuracy of the numerical solution for the transformed temperature dependence on time has been established, it is possible to evaluate the series solution convergence. Since steady-state eq. (27) was utilized as filter in eq. (26), convergence of the series solution gets increasingly worse as the initial state is approached. Hence, a conservative analysis is performed here by evaluating the series solution convergence at $t = 0.0001$. This is illustrated in fig. 6 with $N = 10, 20, \ldots, 50$ for the thermodynamic conditions reported in (a) fig. 1, where $\gamma_0 \approx 5$, and (b) fig. 3, where $\gamma_0 \approx 15.5$. The $N = 90$ solution is this figure is close to graphical convergence at both times. In fact, estimated error relative to the maximum temperature difference at $t = 0.0001$, 0.001, 0.01, 0.1, and 1 is 0.37, 0.28, 0.17, 0.022, and 0.0%, for fig. 1 conditions, and 0.18, 0.048, 0.0069, 0.034, and 0.0%, for fig. 3 conditions. Relative error did not increase with γ_0 when the piston effect got stronger. Nevertheless, in order to guarantee graphical convergence of all results presented next, $N = 100$ is employed.

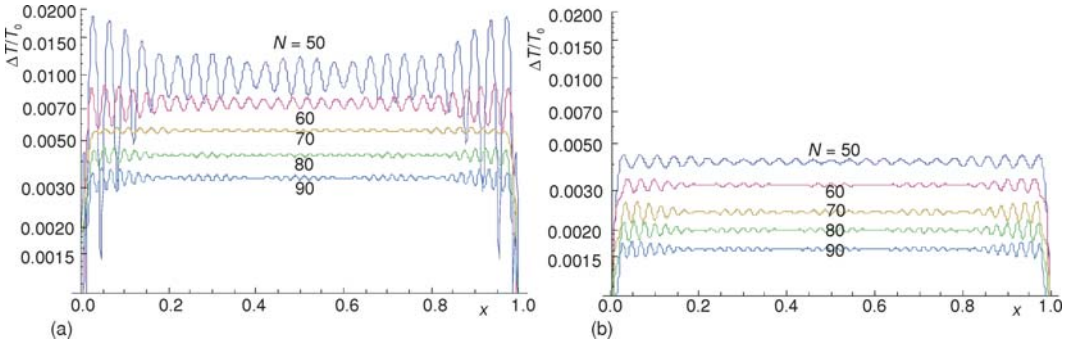

Figure 6. Estimated absolute errors of series solutions with $N = 50$, 60, 70, 80, and 90 at $t = 0.0001$ for the thermodynamic conditions in (a) fig. 1 and (b) fig. 3

Non-linear piston effect

Having finished the solution accuracy verification process, it is now possible to analyze solution behavior. As already mentioned, the main focus of the present study is to better un-

derstand the impact that property dependence on temperature and pressure has on the piston effect using the GITT. In order to provide additional information to the only other such study found in [12], temperature and pressure differences imposed do not force to fluid across pseudo-critical lines. In other words, property dependence on temperature and pressure is always monotonic. Furthermore, they are linearized around a reference state and vary up to 30% with temperature and pressure, as shown in figs. 1 to 4. Temperature variations across the cavity at different times are presented in fig. 7 for constant (dashed lines), temperature dependent only (dotted) as well as temperature and pressure dependent (solid lines) properties when subjected to all four conditions considered in previous figures. Maximum differences between all three lines are less than 2.5% and occur at intermediate times, consistent with the earlier study [12]. Figures 1 to 4 imply that any property increase (decrease) caused by the imposed temperature difference is essentially cancelled out by an equivalent decrease (increase) caused by the induced pressure difference. However, temperature profiles essentially do not change when one considers only temperature dependent properties, *i. e.*, properties without any pressure dependence. This result indicates that the thermo-acoustic heating process, which gets stronger as the critical point is approached, depends on the initial pressure wave generated when both boundary temperatures are increased from T_0 to T_1 at $t = 0^+$. Recent direct numerical simulations of acoustic waves, generated with transient boundary heating as fast as a few acoustic characteristic times, support this conclusion [23]. The present work goes a step further, indicating that subsequent property variations, *i. e.*, after $t > 0^+$, do not significantly affect the propagation and reflection of this wave.

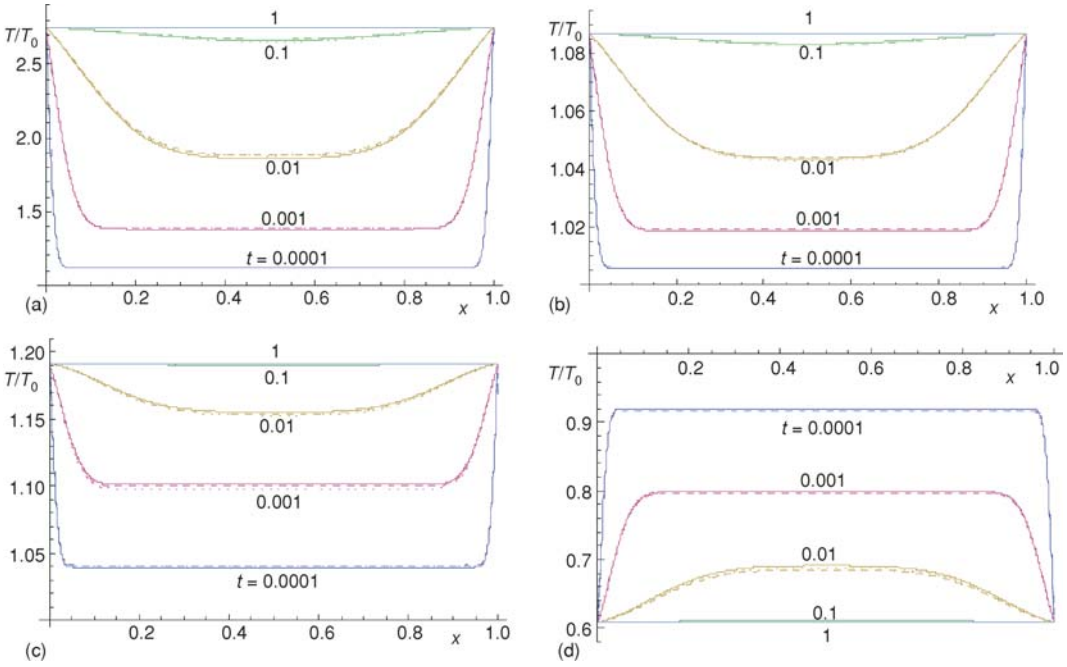

Figure 7. Temperature field for the conditions described in (a) fig. 1, (b) fig. 2, (c) fig. 3, and (d) fig. 4 for variable (solid), temperature dependent only (dotted) and constant (dashed) property cases

Conclusions

The present study considers the unsteady heat transfer occurring in a compressible fluid under micro-gravity and near its thermodynamic critical point, allowing for all properties to depend on both temperature and pressure. It shows that the GITT is also able to capture the non-linear piston effect. Furthermore, it demonstrates that initial conditions are the most important factor controlling thermo-acoustic heating, since property variations have negligible effect. Hence, the constant property assumption is valid and can be used to model the piston effect under a wide range of temperature and pressure variations.

References

[1] Carles, P., A Brief Review of the Thermophysical Properties of Supercritical Fluids, *The Journal of Supercritical Fluids, 53* (2010), 1, pp. 2-11
[2] Nitsche, K., Straub, J., The Critical Hump of C_V under Microgravity, Results from d-Spacelab Experiment, *Proceedings*, 6th European Symposium on Material Sciences under Microgravity Conditions, ESA, Paris, ESA SP-256, 1987, pp. 1-9
[3] Onuki, A., *et al*., Fast Adiabatic Equilibration in a Single-Component Fluid Near the Liquid-Vapor Critical Point, *Physical Review A, 41* (1990) 4, pp. 2256-2259
[4] Boukari, H., *et al*., Critical Speeding up in Pure Fluids, *Phys. Rev. A, 41* (1990), 4, pp. 2260-2263
[5] Onuki, A., Ferrell, R. A., Adiabatic Heating Effect Near the Gas-Liquid Critical Point, *Physica A, 164* (1990), 2, pp. 245-264
[6] Zappoli, B., *et al*., Anomalous Heat Transport by the Piston Effect in Supercritical Fluids under Zero Gravity, *Physical Review A, 41* (1990), 4, pp. 2264-2267
[7] Ferrell, R. A., Hao, H., Adiabatic Temperature Changes in a One-Component Fluid Near the Liquid-Vapor Critical Point, *Physica A, 197* (1993), 1-2, pp. 23-46
[8] Garrabos, Y., *et al*., Relaxation of a Supercritical Fluid After a Heat Pulse in the Absence of Gravity Effects: Theory and Experiments, *Physical Review E, 57* (1998), 5, pp. 5665-5681
[9] Carles, P., *et al*., Temperature and Density Relaxation Close to the Liquid-Gas Critical Point: An Analytical Solution for Cylindrical Cells, *Physical Review E, 71* (2005), 4, p. 041201
[10] Alves, L. S. de B., Unsteady Compressible Heat Transfer in Supercritical Fluids, *Proceedings*, ENCIT2012-347, 14th Brazilian Congress of Thermal Sciences and Engr., Rio de Janeiro, RJ, Brazil, 2012, pp. 1-9
[11] Teixeira, P. C., Alves, L. S. de B., Piston Effect Characteristic Time Dependence on Equation of State Model Choice, CHT-12-EN02, Int. Symp. on Adv. in Comp. Heat Transfer, Bath, England, 2012, pp. 1-11
[12] Masuda, Y., *et al*., One Dimensional Heat Transfer on the Thermal Diffusion and Piston Effect of Supercritical Water, *International Journal of Heat and Mass Transfer, 45* (2002), 17, pp. 3673-3677
[13] Zappoli, B., The Response of a Nearly Supercritical Pure Fluid to a Thermal Disturbance, *Physics of Fluids, 4* (1992), 5, pp. 1040-1048
[14] Carles, P., Zappoli, B., The Unexpected Response of Near-Critical Fluids to Low-Frequency Vibrations, *Physics of Fluids, 7* (1995), 11, pp. 2905-2914
[15] Carles, P., The Effect of Bulk Viscosity on Temperature Relaxation Near the Critical Point, *Physics of Fluids, 10* (1998), 9, pp. 2164-2176
[16] Cotta, R. M., *Integral Transforms in Computational Heat and Fluid Flow*, CRC Press, Boca Raton, Fla., USA, 1993
[17] Özisik, M. N., *Heat Conduction*, 2nd ed., Wiley Interscience, New York, USA, 1993
[18] Cotta, R. M., The Integral Transform Method in Thermal and Fluids Science and Engineering, Begell House, Inc., New York, USA, 1998
[19] Alves, L. S. de B., Cotta, R. M., Transient Natural Convection Inside Porous Cavities: Hybrid Numerical-Analytical Solution and Mixed Symbolic-Numerical Computation, *Numerical Heat Transfer*, *Part A – Applications, 38* (2000), 1, pp. 89-110
[20] Alves, L. S. de B., *et al*., Covalidation of Hybrid Integral Transforms and Method of Lines in Nonlinear Convection-Diffusion with Mathematica, *Journal of the Brazilian Society of Mechanical Sciences, 23* (2001), 3, pp. 303-320
[21] Alves, L. S. de B., *et al*., Stability Analysis of Natural Convection in Porous Cavities through Integral Transforms, *International Journal of Heat and Mass Transfer, 45* (2002), 6, pp. 1185-1195

[22] Wolfram, S., *The Mathematica Book*, 5th ed., Wolfram Media, Cambridge University Press, New York, USA, 2003
[23] Shen, B., Zhang, P., On the Transition from Thermoacoustic Convection to Diffusion in a Near-Critical Fluid, *International Journal of Heat and Mass Transfer, 53* (2010), 21-22, pp. 4832-4843

Paper submitted: August 26, 2012
Paper revised: April 24, 2013
Paper accepted: May 24, 2013